Elucidating the role of CO in NO storage mechanism on Pd/SSZ-13 with *in situ* DRIFTS

Inhak Song,[a] Konstantin Khivantsev,[a]* Yong Wang,[a,b] and János Szanyi[a]*

[a]Institute for Integrated Catalysis, Pacific Northwest National Laboratory, Richland, Washington 99352, United States

[b]Voiland School of Chemical Engineering and Bioengineering, Washington State University, Pullman, Washington 99164, United States

*Corresponding authors: konstantin.khivantsev@pnnl.gov and janos.szanyi@pnnl.gov

Abstract

Pd ion exchanged zeolites emerged as promising materials for the adsorption and oxidation of air pollutants. For low-temperature vehicle exhaust, dispersed Pd ions are able to adsorb NO_x even in H_2O-rich exhaust in the presence of carbon monoxide. In order to understand this phenomenon, changes in Pd ligand environment have to be monitored in-situ. Herein, we directly observe the activation of hydrated Pd ion shielded by H_2O into a carbonyl-nitrosyl complex $Pd^{2+}(NO)(CO)$ in SSZ-13 zeolite. The subsequent thermal desorption of ligands on $Pd^{2+}(NO)(CO)$ complex proceeds to nitrosyl Pd^{2+} rather than to carbonyl Pd^{2+} under various conditions. Thus, CO molecules act as additional ligands to provide alternative pathway through $Pd^{2+}(NO)(CO)$ complex with lower energy barrier for accelerating NO adsorption on hydrated Pd^{2+} ion, which is kinetically limited in the absence of CO. We further demonstrate that hydration of Pd ions in the zeolite is a prerequisite for CO-induced reduction of Pd ions to metallic Pd. The reduction of Pd ions by CO is limited under dry conditions even at a high temperature of 500°C, while water makes it possible at near RT. However, the primary NO adsorption sites are Pd^{2+} ions even in gases containing CO and water. These findings clarify additional mechanistic aspects of the passive NO_x adsorption (PNA) process and will help extend the NO_x adsorption chemistry in zeolite-based adsorbers to practical applications.

1. Introduction

The global air pollution crisis poses a substantial challenge for the automotive industry to develop improved emission technologies.[1-2] Current and future regulations aim for nearly zero emissions, which requires the development of effective technologies for NO_x abatement during the cold start period of a vehicle operation. Current NO_x control for lean-burn diesel exhaust is achieved by either NO_x storage and reduction (NSR) catalysts or selective catalytic reduction (SCR) catalysts using urea as the reducing agent.[3-5] Unfortunately, both technologies are ineffective for NO_x abatement at temperatures below 200°C due to the slow oxidation of NO to NO_2, the unsatisfactory activity of NO reduction, incomplete decomposition of urea to gaseous NH_3, and the potential deactivation due to ammonium-nitrate salts deposition.[6-10]

One feasible strategy is passive NOx adsorption (PNA), which traps NO_x at low temperatures and releases it thermally at high temperatures where NSR or SCR catalysts start working. Johnson Matthey Inc. first reported the potential of zeolite supported Pd catalysts as efficient NO storage materials.[11] Unlike CeO_2 supported Pd, which is severely deactivated with sulfur,[12] the exchanged Pd ions located inside the zeolites retain their NO storage capacities even after sulfation. (Our recent study on single Ru site for NO storage revisited the potential of CeO_2-based materials for industrial application.[13]) Subsequent multiple studies commonly showed that highly dispersed Pd^{2+} ions in cationic positions of zeolites are the sites for NO adsorption.[14-16] Until recently, Pd/zeolite materials have been actively studied not only as a NOx adsorber but also as a catalyst for oxidation of unburned methane and carbon monoxide.[17-19]

Initially, researchers focused on how Pd could be well dispersed in small pore zeolites to increase NO storage capacity with maximum atom efficiency. Although small pore zeolites with excellent hydrothermal stability were justly preferred as supports for PNA materials,[20] it was difficult to disperse Pd ions within zeolites due to the clustering of PdO species. Our studies, in which we systematically altered the Si to Al ratio of SSZ-13 zeolites established that hydrophilic, i.e., Al-rich zeolites, were preferred for dispersing Pd^{2+} ions without formation of large PdO clusters.[21] In addition, coordination of Pd^{2+} ions with NH_3 ligands in precursor solution was found to be essential for achieving high dispersion in incipient wetness impregnation method. One of the interesting properties of supported Pd materials is the dynamic nature of Pd active species, which is usually accompanied by significant changes in their dispersion.[22-26] Such changes originate from transformation between PdO and Pd phase depending on oxidizing or reducing atmosphere and the presence of anchoring sites for certain Pd species. For example, agglomerated PdO on the external surface can reversibly disperse into the zeolite with high temperature treatment, which is believed to be driven by the interaction between acid sites of zeolite and basic PdO.[27] Ryou et al. observed that hydrothermal aging of Pd/SSZ-13 containing PdO could redisperse PdO to Pd^{2+} ions within the zeolite structure.[28] Our earlier work, however, have shown that hydrothermal aging of Pd/zeolites containing

dominantly Pd^{2+} ions resulted in the formation of PdO clusters.[29] This shows that the distribution of PdO and Pd determined by hydrothermal treatment is strongly influenced by the initial state of Pd. In fact, a recent study demonstrated that high temperature treatment without water is also effective in redispersing PdO into Pd^{2+} ions in SSZ-13 zeolites.[30] Interestingly, our recent study observed that high temperature treatment could not only disperse PdO but also affect the distribution of Pd^{2+} ions in FER zeolites.[18]

Dispersed Pd^{2+} ions anchored at negatively charged AlO_4^- sites within the zeolite frameworks are known to effectively adsorb NO under dry conditions. Under wet conditions, however, the ratio of adsorbed NO to Pd drastically decreases due to the competitive coordination of H_2O molecules to Pd^{2+} ions.[14] Our earlier work found that the addition of CO improved the PNA storage capacity of Pd/SSZ-13 in the presence of H_2O, which was explained by the formation of a carbonyl-nitrosyl complex, i.e., $Pd^{2+}(NO)(CO)$.[15] This complex was consistently observed for other Pd/zeolites, including BEA, SSZ-39, and FER, and was suggested to be responsible for NO storage with the aid of static IR.[17-18, 31] Meanwhile, several studies raised the possibility that the reducing effect of CO on Pd^{2+} ions could be responsible for promotion of NO adsorption by CO.[32-34] The existence of $Pd^{2+}(NO)(CO)$ complex under practical conditions was also observed: however, some groups observed the complex but some did not in the *in situ* DRIFTS experiments.[35-37]

In this study, we performed systematic diffuse reflectance infrared Fourier transform spectroscopy (DRIFTS) measurements over Pd/SSZ-13 materials to understand how CO promotion occurs during NO adsorption and to elucidate the role of $Pd^{2+}(NO)(CO)$ complex in passive NO_x adsorption. The issues to be addressed in this work include the following clarifications: (i) whether the $Pd^{2+}(NO)(CO)$ complex actually present at temperatures near 100°C in Pd/SSZ-13 under the simulated exhaust gas or not, and (ii) how the state of Pd^{2+} ions can change upon exposure to H_2O, NO, and CO. Valuable information was obtained by comparing the absorption spectra for hydrated Pd/SSZ-13, which has condensed water in its micropore, to those for "normal" dehydrated Pd/SSZ-13 pretreated at high temperatures. This work contributes to the understanding of the state of Pd ions and their coordination environment in the zeolite framework, which is necessary for designing efficient NO_x storage materials for practical applications.

2. Experimental methods

The Pd/SSZ-13 material used throughout this work is the same material whose preparation method was detailed in our previous studies.[21, 29] Briefly, NH_4-SSZ-13 with Si to Al ratio of 6 was prepared by hydrothermal synthesis of Na-SSZ-13 and its subsequent ion-exchange with NH_4NO_3 aqueous solution. Pd/SSZ-13 with 3 wt.% Pd loadings were prepared by modified ion exchange method using an aqueous 10

wt.% tetraamminepalladium(II) nitrate solution. A minimum amount of the Pd precursor solution was added to the NH_4-zeolite in the amount equivalent to the micropore volume of the zeolite. The thick paste was mixed and stirred vigorously followed by calcination in air at 700°C for 5 h with the ramping rate of 2°C/min. Sample stored in vial was thermally treated at 700°C for 1 h in static oven to oxidize any impurities before DRIFTS experiments and stored in vial again in ambient conditions.

The *in situ* diffuse reflectance IR measurements were performed in a commercial praying mantis DRIFTS cell with ZnSe window. The IR spectra were collected on Nicolet iS50 FT-IR (Thermo Fisher Scientific Co., USA) spectrometer equipped with a liquid nitrogen-cooled MCT detector. Each spectrum was obtained as the average of 32 scans with 4 cm^{-1} resolution. A background spectrum was recorded with KBr powder at temperatures where measurements were conducted. The space through which the IR beam passes on both sides of the reactor window was continuously purged with nitrogen to maintain a constant background. In a typical experiment, the body of the sample cup was filled with α-alumina powder. Then, a thin layer of sample was spread over it and pressed firmly. Gas stream through the DRIFTS cell was controlled by mass flow controllers. The outlet of the DRIFTS cell was connected to a quadrupole mass spectrometer (Hiden Analytical). For dehydration of the zeolite, the cell was heated to 450°C with the ramping rate of 10°C/min and held at 450°C for 30 min in 1.5% O_2/He flow. When conducting gas adsorption on hydrated zeolite, the sample was only heated to the target temperature (usually 100°C) and held for 30 min without any additional thermal treatment. H_2O was injected by flowing the gas through a glass bubbler filled with distilled water. The concentration of water was controlled by varying temperature of bubbler from 0°C to RT.

3. Results and discussion

3.1. Formation of $Pd^{2+}(NO)(CO)$ complex under dry condition

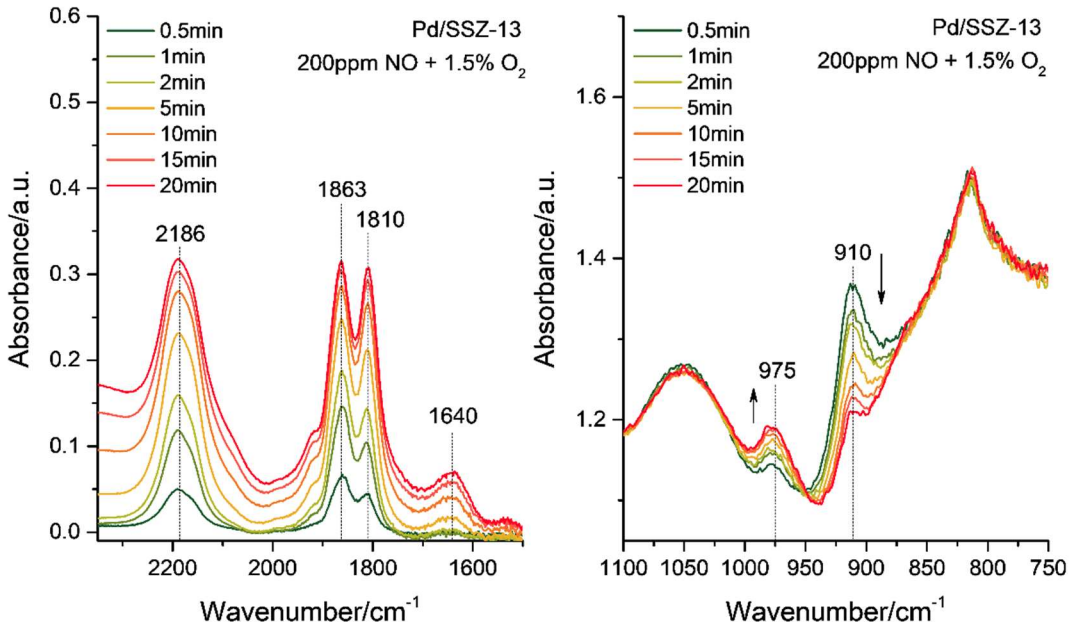

Figure 1. Series of DRIFT spectra collected after exposure of dehydrated (450°C under 1.5% O_2) Pd/SSZ-13 to 200ppm NO + 1.5% O_2 at 100°C.

The Pd/SSZ-13 sample kept in ambient air is always fully hydrated due to the hydrophilic nature of the zeolite framework (Si/Al~6).[38] The sample was pretreated at high temperature before gas adsorption measurement to remove H_2O molecules coordinated onto Pd^{2+} ions. IR spectra of the Pd/SSZ-13 obtained at 100°C before and after dehydration are shown in Figure S1. The broad band in the range of 2200 to 3800 cm^{-1} represents the various OH groups contained in zeolite, including silanols and zeolitic OH groups that interact with H_2O molecules via hydrogen bonding.[38-39] A distinct IR band centered at 1630 cm^{-1} is the bending mode of adsorbed H_2O. The dehydration process clearly removes these features of adsorbed water. Another noticeable change caused by dehydration is the conversion of a relatively broad band near 924 cm^{-1} to a sharp band at 910 cm^{-1}. Both bands are related to the presence of Pd^{2+} ions because they are not observed in H/SSZ-13. In fact, this change is quite analogous to the case of Cu ion-exchanged SSZ-13 zeolite as described in our prior work.[38] It has been reported that certain framework vibrational modes, ν(T-O-T), of zeolites are sensitive to the charge compensating cations, thereby inducing perturbed vibrational features located between 850 and 950 cm^{-1}.[40-41] The perturbation band of hydrated Cu^{2+} ions appears around

950 cm^{-1} for the case of Cu/SSZ-13, while it gradually changes to intense feature of naked Cu^{2+} ion near 900 cm^{-1} with dehydration. Although the exact reason of such intensity variations of the framework vibrations are not clearly understood, we tentatively assign the band around 924 cm^{-1} to T-O-T vibrations perturbed by hydrated Pd^{2+} ions and the band at 910 cm^{-1} to naked Pd^{2+} ions closely interacting with the negatively charged framework.

NO adsorption in the presence of oxygen was conducted over dehydrated Pd/SSZ-13 by flowing a 200 ppm NO + 1.5 % O_2 mixture at 100°C (Figure 1). Exposure to this gas stream for 20 min was sufficient to reach adsorption equilibrium under these conditions. The typical two sharp nitrosyl bands at 1863 and 1810 cm^{-1} grew rapidly, which were previously assigned to the N-O vibrations in Pd^{2+}-NO and Pd^{+}-NO complexes, respectively.[15, 42] The broad band centered at 2186 cm^{-1} represents nitrosonium ions (NO^{+}) formed by the replacement of Brønsted acid sites (H^{+}) in the zeolite.[43] Such oxidation of NO to NO^{+} should be coupled with the reduction of Pd^{2+} to Pd^{+} or the reduction of O_2 to H_2O. In fact, the peak of adsorbed H_2O at 1640 cm^{-1} and broad band from 2200 to 3800 cm^{-1} increase with NO adsorption, which indicates the formation of H_2O. There is general agreement that the peak at 1863 cm^{-1} represents chemisorbed NO on cationic Pd^{2+} sites,[15, 28, 35, 42] but it is quite complex to find the origin of the band at 1810 cm^{-1}. Our earlier static IR results on Pd/SSZ-13 under exclusively moisture-free conditions showed that pulses of NO initially lead to the appearance of only the 1865 cm^{-1} band: Its decrease within very short time coincides with the appearance and increase of intensity of the bands at 1805 and 2160 cm^{-1}.[42] Such decrease in Pd^{2+}-NO accompanied by NO^{+} formation implies that the 1805 cm^{-1} feature is related to Pd^{+}-NO. This is a definitive proof that NO radical is able to transfer its free electron to the redox-active metal situated in the zeolite, be it Pd(II) or Cu(II).[44] Interestingly, a recent study on Pd/SSZ-39 showed the increase of 1810 cm^{-1} feature without the formation of NO^{+} species, which suggests the possible assignment of 1810 cm^{-1} feature as Pd^{2+}(OH)NO.[17] Mandal *et al.* also suggested that the band at 1818 cm^{-1} on Pd/SSZ-13 was related to hydration of Pd^{2+} ions in the presence of water.[35] This implies that various kinds of NO species have similar N-O frequencies in the 1810±10 cm^{-1} wavenumber region. The band of framework vibration perturbed by Pd^{2+} ions at 910 cm^{-1} gradually decreases in intensity with NO adsorption. The peak at 975 cm^{-1} appeared at the same time, which can tentatively be assigned as perturbed framework vibration by Pd^{2+}-NO. Similar perturbation of divalent cation with coordinating molecule was previously observed for Co-ion exchanged ferrierite.[41] It is worth noting that the perturbation peak of the naked Pd^{2+} ion does not completely disappear even after NO adsorption for 20min. The small remaining peak disappears quickly only when CO is added to the NO stream (Figure 2b), indicating the interaction between the Pd^{2+} ions and the framework is weakened.

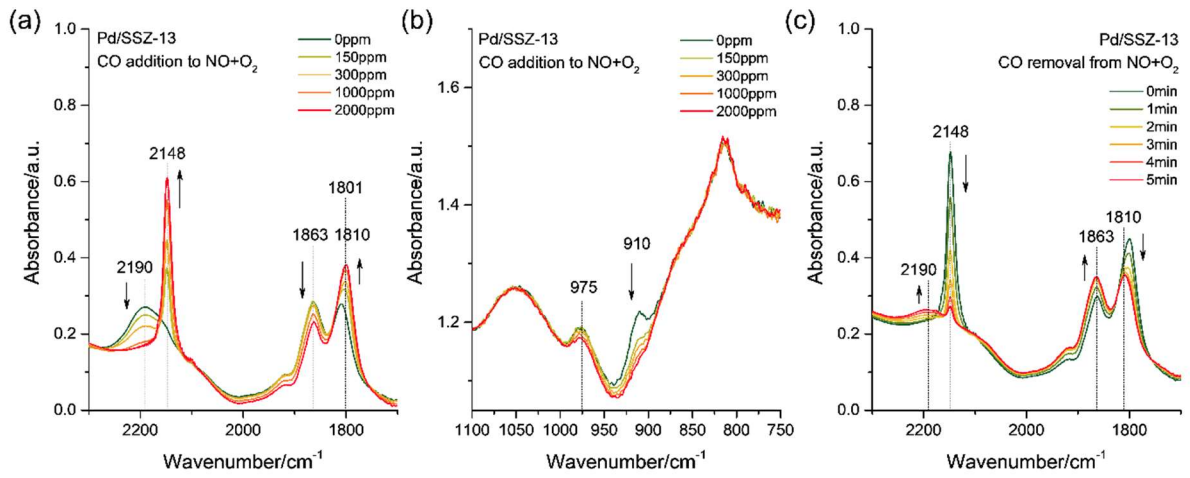

Figure 2. Series of DRIFT spectra collected from dehydrated (450°C under 1.5% O_2) Pd/SSZ-13 at 100°C. After pre-adsorption of 200ppm NO + 1.5% O_2, (a, b) the sample was exposed to CO with varying concentration from 150 to 2000 ppm. (c) Then, CO was removed from the NO+O_2 feed.

The addition of CO leads to the formation of Pd^{2+}(NO)(CO) complex evidenced by the development of IR features at 2148 and 1801 cm^{-1} (Figure 2a). As the CO concentration increases from 150 to 2000 ppm, the amount of Pd^{2+}(NO)(CO) increases with a decrease in the Pd^{2+}-NO peak at 1863 cm^{-1}. This observation is consistent with our previous data obtained from static FTIR experiments.[15] One interesting observation is the behavior of the NO^+ band at 2190 cm^{-1}, which gradually diminishes with increasing CO pressure. Considering that no adsorbed CO was found when flowing CO on bare H-zeolite at 100°C, the above phenomenon cannot be the simple replacement of NO^+ with CO-related adsorbates. One possibility is that desorption of NO^+ species to NO and NO_2 are facilitated with a trace amount of H_2O contained in CO gas, i.e., $2NO^+ + H_2O \rightarrow 2H^+ + NO + NO_2$. When CO is removed from the NO+O_2 stream, the Pd^{2+}(NO)(CO) complex progressively decomposes and the Pd^{2+}-NO peak is fully restored (Figure 2c). Note that an identical trend was also observed under vacuum condition in the static IR experiments.[15] First, this observation shows different binding strengths of NO vs. CO ligands in Pd^{2+}(NO)(CO) complex under these conditions, consistent with earlier findings that NO, unlike CO, does not adsorb linearly and chemisorbs with the formation of a full sigma-bond via coupling of its unpaired electron with Pd electron and assuming a bent configuration.[45] Second, Pd^{2+}-NO peak is exactly the same before and after CO addition, which means that CO does not replace NO bound to Pd^{2+} ions, and CO does not reduce Pd^{2+} ions.

3.2. Effects of CO on NO adsorption in hydrated Pd/SSZ-13

A series of experiments for dehydrated Pd/SSZ-13 ascertain the presence of Pd^{2+}(NO)(CO) complex on naked Pd^{2+} ions. Identical experiments were performed on hydrated Pd/SSZ-13 without thermal treatment: it is established that in this case most of the Pd^{2+} ions are coordinated with water condensed in the micropores. In these experiments, Pd/SSZ-13 loaded in the DRIFTS cell was heated up to 100°C and held for 35 min under 1.5% O_2/He flow (Figure S2). With a slight decrease in the 3000 to 3500 cm^{-1} band, the features of the Fermi resonance between adsorbed water molecules and hydroxyl groups in framework at 2400 and 3000 cm^{-1} becomes more distinct at 100°C.[39] Also, the perturbation of hydrated Pd^{2+} ions at 942 cm^{-1} shifted to 915 cm^{-1} with a slight decrease. These overall changes indicate that some of the physically adsorbed water inside the micropores adjacent to hydrated Pd^{2+} ions was desorbed at 100°C. Compared to the spectra of fully dehydrated samples (Figure S1), however, it is obvious that most of the water is still present in the zeolite after holding the sample at 100°C for 35 min.

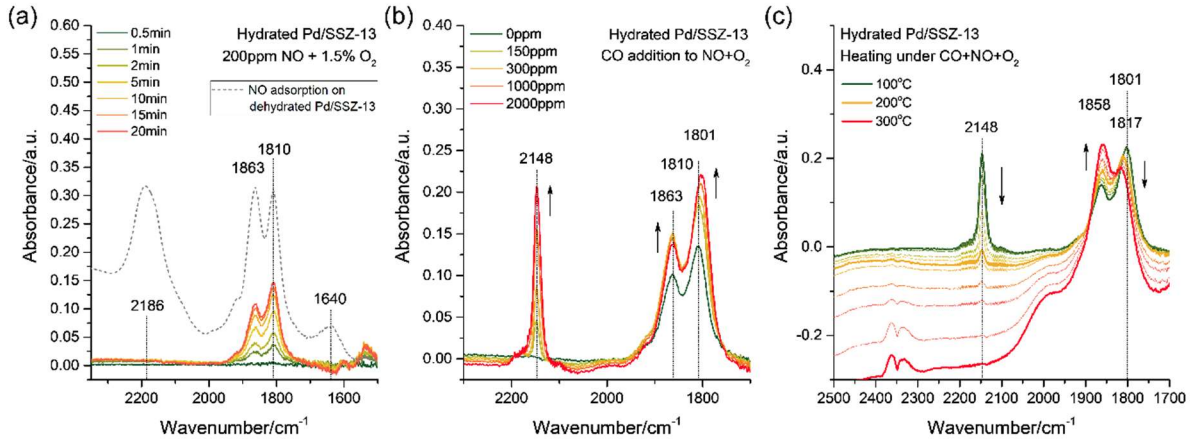

Figure 3. Series of DRIFT spectra collected for hydrated Pd/SSZ-13 at 100°C without dehydration. (a) Spectra obtained during adsorption of 200ppm NO + 1.5% O_2 at 100°C. Subsequently, (b) sample was exposed to CO with varying concentration from 150 to 2000 ppm. (c) Then, sample was heated to 300°C under CO+NO+O_2 flow.

The amount of adsorbed NO on hydrated zeolite dropped to less than half of the dehydrated zeolite (Figure 3a). Such limited NO adsorption occurs because H_2O molecules shielding Pd^{2+} ions make it difficult for the NO molecules to coordinate. This may be due only to kinetic limitations, which is attributed to high concentration of H_2O compared to NO, because the binding of Pd^{2+}-NO is thermodynamically more stable than Pd^{2+}-H_2O as calculated in our earlier work.[42] The absence of the NO^+ band near 2186 cm^{-1} is the result of strong coordination of H_2O to Brønsted acid sites. The 1640 cm^{-1} band of H_2O no longer grows during NO adsorption, for the same reason. The addition of 150 ppm CO abruptly increases the intensities of both Pd^{2+}-NO bands, consistent with the observed increase in NO_x storage in the presence of CO in typical PNA

experiments (Figure 3b). This clearly demonstrates that the presence of CO promotes NO storage in the form of Pd^{2+}-NO and not Pd^{+}-NO. Interestingly, at the low CO partial pressure of 150 ppm large increases in the intensities of the Pd^{2+}-NO bands at 1863 and 1810 cm^{-1} is observed primarily. When the CO pressure was increased to 1000 ppm the intensity of the 1863 cm^{-1} feature decreased concomitant with an increase of the 1801 cm^{-1} band, evidencing the formation of the Pd^{2+}(NO)(CO) complex (2148, 1801 cm^{-1}). After co-adsorption of NO and CO, the cell was heated from 100 to 300°C while maintaining the NO, CO, and oxygen flows (Figure 3c). The Pd^{2+}(NO)(CO) complex is easy to decompose reflecting its low stability at elevated temperature (the intensity of the 2148 cm^{-1} IR feature decreased dramatically as the sample temperature reached 200°C). The base line shift above 2000 cm^{-1} is related to the desorption of water. Such dehydration produces more "naked" Pd^{2+} ions, resulting in a transient increase in the Pd^{2+}-NO band at 1858 cm^{-1}.

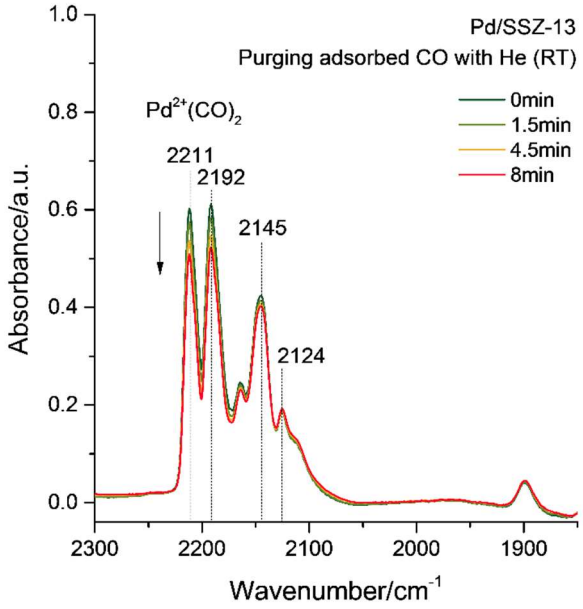

Figure 4. Series of DRIFT spectra collected at RT for re-oxidized (450°C, 1.5% O_2) Pd/SSZ-13. Sample was purged with He after CO adsorption under 2000ppm CO + 1.5% O_2.

3.3. Conversion of Pd^{2+}-carbonyl to Pd^{2+}(NO)(CO) complex

After re-oxidizing the Pd/SSZ-13 sample under 1.5 % O_2 at 450°C, the cell was cooled to ambient temperature for CO adsorption (Figure 4). The most intense peaks located at 2211 and 2192 cm^{-1} represent dicarbonyl complexes of Pd^{2+} ions.[42] These high wavenumber features have previously been assigned to

dicarbonyl Pd^{3+} species.[46] Our recent study, however, established that the negatively charged zeolite framework acts as a weakly coordinating macroligand to naked super-electrophile Pd^{2+} that makes the C-O stretching vibration of the Pd^{2+}-dicarbonyl species appear at extremely high wavenumbers.[42] Peaks at 2145 and 2124 cm^{-1} are assigned to $Pd^{2+}(OH)(CO)$ species, which are charge compensating 1Al sites. Note that $Pd^{2+}(CO)_2$ cannot be observed when the Pd/SSZ-13 is exposed to 2000ppm CO at 100°C, because it is thermally rather unstable. Purging the cell with He after CO adsorption results in the gradual (slow) decomposition of Pd^{2+}-dicarbonyl species.

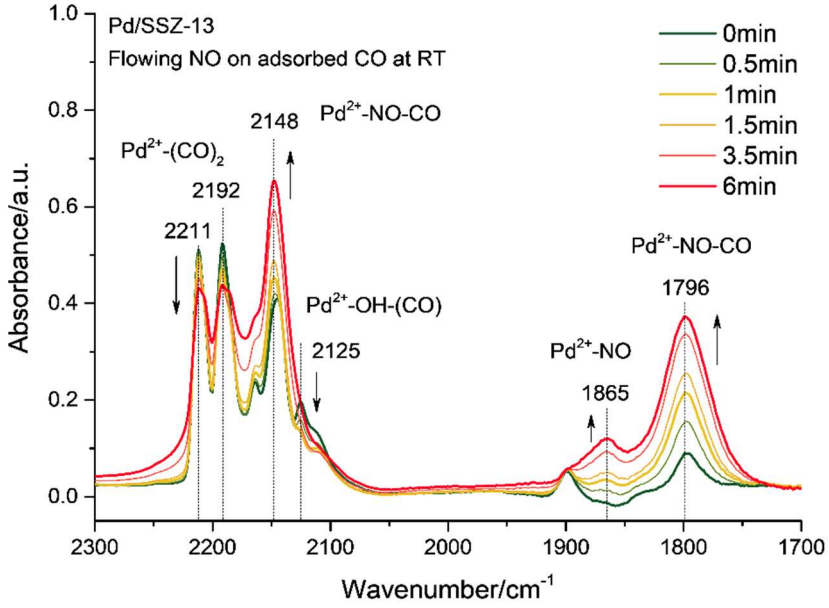

Figure 5. Series of DRIFT spectra collected for re-oxidized (450°C, 1.5% O_2) Pd/SSZ-13. 200ppm NO was added to the sample after CO adsorption under 2000ppm CO + 1.5% O_2 at RT and subsequent He purging.

After CO adsorption and subsequent He purge, 200 ppm NO was introduced into the IR cell (Figure 5). The introduction of NO onto the CO-saturated Pd/SSZ-13 sample resulted in the fast intensity increase of the 1796 cm^{-1} feature that has been assigned to the N-O vibration of the mixed-ligand $Pd^{2+}(CO)(NO)$ complex. Concomitantly, the intensity of the doublet feature (2192-2211 cm^{-1}) of the $Pd^{2+}(CO)_2$ species decreased while that of the 2148 cm^{-1} band increased, indicating the conversion of the dicarbonyl complex to the mixed-ligand carbonyl-nitrosyl complex. At longer NO exposure time the 1865 cm^{-1} IR feature of $Pd^{2+}(NO)$ also increased. This can be explained by the slow, but continuous desorption of CO from the Pd^{2+} adsorption sites, and/or by the oxidation of Pd(0) sites in the presence of NO to Pd^{2+} and the subsequent NO adsorption of the sites thus created (This may be substantiated by the disappearance of the IR band at

~1900 cm^{-1} assigned to metallic Pd-adsorbed CO species). We conducted similar experiment at 100°C to see whether the conversion of carbonyl Pd^{2+} can occur under PNA condition (Figure S3). In fact, the conversion of Pd^{2+}-carbonyl to Pd^{2+}(NO)(CO) complex was much faster (completed in less than 30s) than at RT. From these observations, we can deduce that once carbonyl Pd^{2+} ions are formed, they will be rapidly converted into Pd^{2+}(NO)(CO) complex under PNA condition. Note that some of the formed Pd^{2+}(NO)(CO) can partially transform into Pd^{2+}-NO in the absence of CO (Figure S3).

3.4. Activation of hydrated Pd^{2+} ions via Pd^{2+}(NO)(CO) route

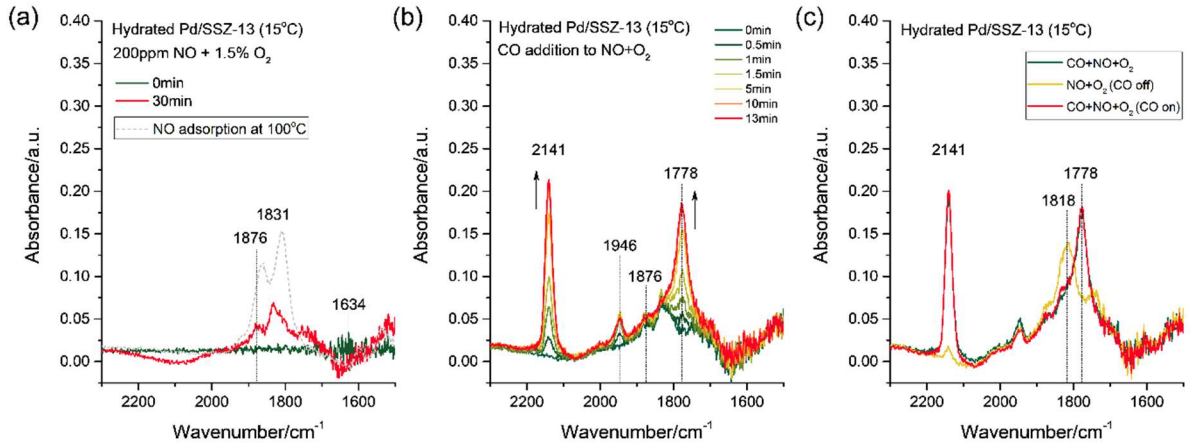

Figure 6. Series of DRIFT spectra collected for hydrated Pd/SSZ-13 at 15°C without dehydration. (a) Spectra obtained during adsorption of 200ppm NO + 1.5% O_2 at 15°C. Subsequently, (b) 1000ppm CO was added to NO+O_2 flow at same temperature, and (c) removal and reintroduction of CO was conducted.

The spectroscopic results presented in Figure 3 confirm the role of CO in accelerating the formation of Pd^{2+}-NO, which is kinetically limited in the presence of H_2O. Our hypothesis is that on hydrated Pd^{2+} ions it is difficult to adsorb NO and form Pd^{2+}-NO, and this process is likely activated by the transient formation of Pd^{2+}(NO)(CO). The reason why Pd^{2+}(NO)(CO) was not the dominantly observed species (Figure 3) is due to its instability as it easily decomposes into Pd^{2+}-NO under PNA condition in the presence of low CO amounts (~200 ppm). To prove this, sequential adsorption of NO and CO on hydrated Pd/SSZ-13 was performed at low temperature (15°C), where the Pd^{2+}(NO)(CO) complex is more stable than at 100°C. Another advantage of the low temperature experiments is that the reduction of Pd^{2+} ions by CO can be minimized.

The amount of NO adsorbed on hydrated zeolite at low temperature was much lower than at 100 °C due to the large amount of moisture in the micropores (Figure 6a vs. results in Figure 3). The IR bands of Pd^{2+}-adsorbed NO are observed at 1876, 1831 cm^{-1} close to those seen at 100 C. Interestingly, addition of CO to the NO+O_2 stream leads to the development of IR features at 2141 and 1778 cm^{-1}. We assign this feature to the hydrated mixed (CO)(NO) complex on Pd^{2+}, i.e., $Pd^{2+}(NO)(CO)(H_2O)_x$ (Figure 6b). This may explain the ~20 cm^{-1} red shift of the N-O vibration (1796 vs 1778 cm^{-1}). This is the first *in situ* observation of the conversion of a hydrated Pd^{2+} ion into a $Pd^{2+}(NO)(CO)$ complex. In contrast to the same experiment conducted at 100°C, the $Pd^{2+}(NO)(CO)$ complex no longer decomposes into Pd^{2+}-NO species. The small band centered at 1946 cm^{-1} is assigned to small metallic Pd clusters, which is formed by the reduction of PdO clusters. Subsequent removal of CO from the gas stream leads to decomposition of the $Pd^{2+}(NO)(CO)$ complex and the appearance of a new peak centered at 1818 cm^{-1} (Figure 6c). This peak can undoubtedly be identified as hydrated Pd^{2+}-NO. Note that similar assignment was also reported in a recent paper although experimental conditions were different from those applied in this study.[35] As shown in these spectra, the promoting effect of CO on NO storage is maintained even after CO is removed, because the role of CO is just to increase the formation rate of Pd^{2+}-NO by providing another pathway via $Pd^{2+}(NO)(CO)$ complex through which Pd^{2+}-NO can be formed. The $Pd^{2+}(NO)(CO)$ complex is completely recovered when CO was reintroduced. This indicates that reversible transformation between hydrated $Pd^{2+}(NO)(CO)$ and hydrated Pd^{2+}-NO is also possible in the presence of water in the zeolite.

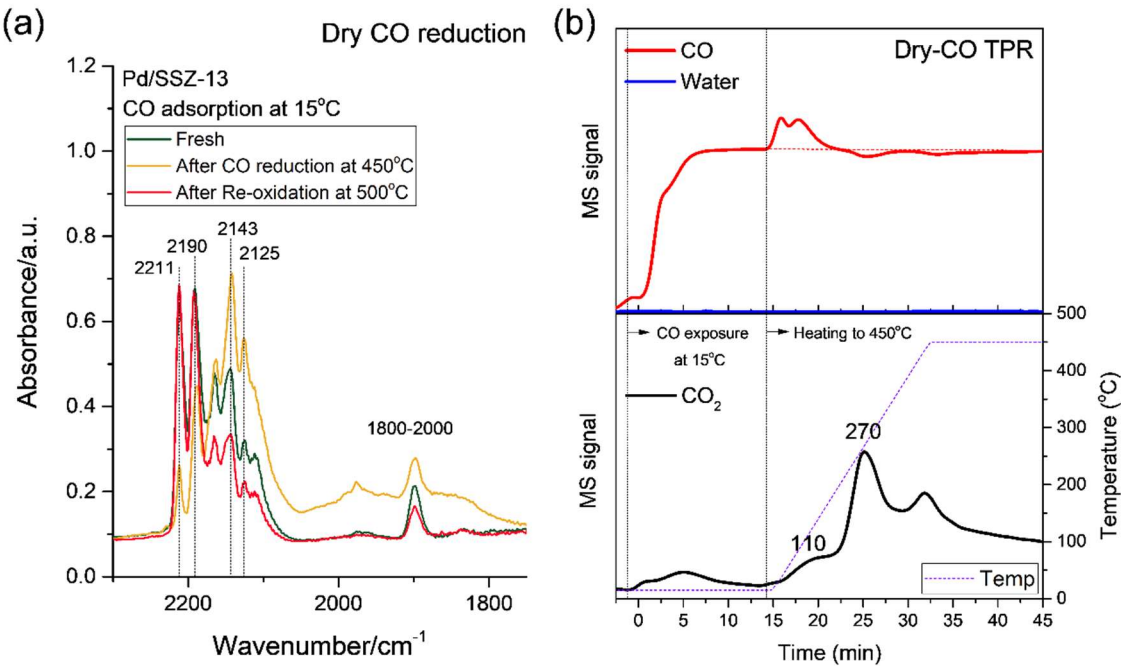

Figure 7. Effect of CO on dehydrated Pd/SSZ-13 was investigated by heating from 15 to 450°C under 2000ppm CO in DRIFTS-MS. (a) Spectra were collected at 15°C after subsequent thermal treatments (1.5% O_2 at 500°C (Fresh), 2000ppm CO at 450°C, and 1.5% O_2 at 500°C again). (b) MS signals for CO and CO_2 during CO reduction for dehydrated Pd/SSZ-13.

Several studies have emphasized the reduction of Pd^{2+} ions in Pd/SSZ-13 by CO and attempted to correlate it with the promoting effect of CO on NO storage.[33-34] To thoroughly examine this possibility, temperature-programmed reduction of Pd/SSZ-13 with CO was performed in the DRIFTS-MS setup (Figure 7). Pd/zeolites usually contain some small PdO clusters inside the zeolite channels and/or at the exterior of zeolite particles, which are hard to detect by bulk technique such as EXAFS and XRD. PdO particles are readily reduced at lower temperatures compared to charge compensating Pd^{2+} ions.[30, 47-48] When dehydrated Pd/SSZ-13 is exposed to CO at 15°C, only slight CO_2 formation was observed probably due to PdO reduction (Figure 7b). The main reduction peak is found around 270°C, which is much higher than the temperature where NO_x uptake is conducted during PNA. Since the promoting effect of CO was still observed even at a low temperature where the reduction of Pd ions does not occur extensively, it seems that the effect of CO has little relation to the reduction of Pd species at least for highly dispersed Pd/SSZ-13 material. One interesting observation is that only a fraction of Pd^{2+} ions is reduced under 2000 ppm CO flow up to 450°C (Figure 7a). The amount of Pd^{2+}-dicarbonyl complex is significantly reduced, while that of Pd^{2+}(OH)(CO) increased. At the same time there is an increase in the -OH intensity at 3605 and 3550 cm^{-1} (Figure S4). Such formation of -OH groups mean there is a trace amount of H_2O in the CO gas although the experiment was conducted under dry condition. In fact, another cation, probably proton (H^+), should be present to charge compensate the zeolite framework after losing Pd^{2+} ions.

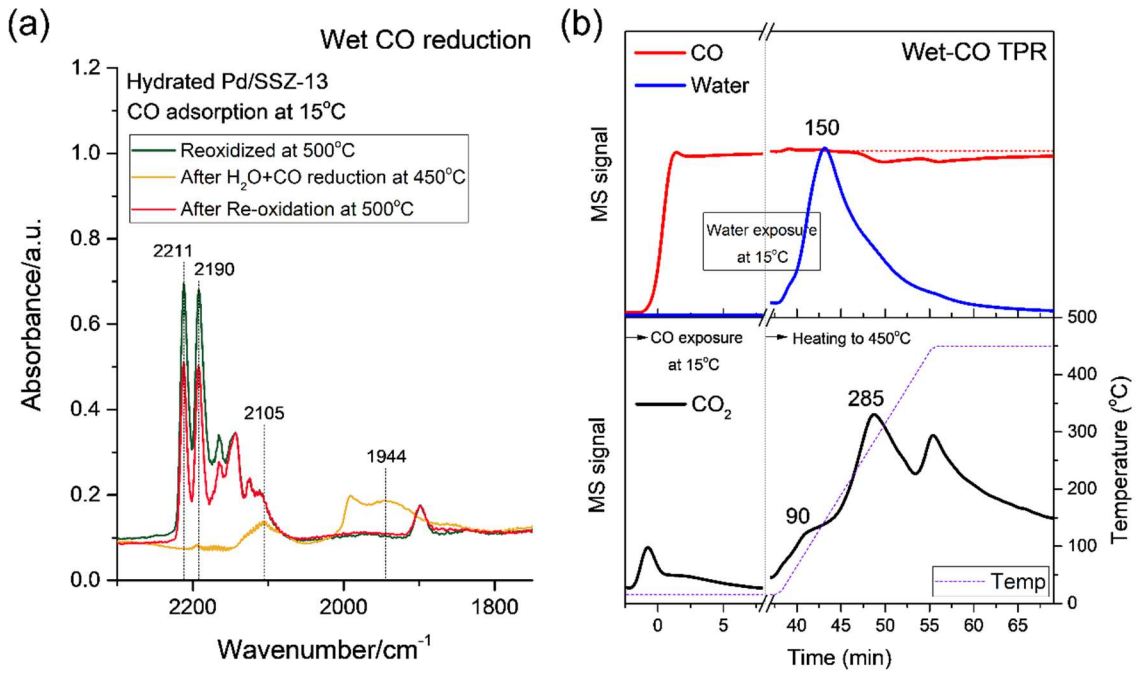

Figure 8. Effect of CO on hydrated Pd/SSZ-13 was investigated by saturating zeolite with water before heating from 15 to 450°C under 2000ppm CO in DRIFTS-MS. Water saturation is conducted by exposing the sample under 2.8% H_2O for 10 min, then subsequently purging with He for 20 min. (a) Spectra were collected at 15°C after subsequent thermal treatments (2000ppm CO at 450°C, and 1.5% O_2 at 500°C). (b) MS signals for H_2O, CO and CO_2 during CO reduction for hydrated Pd/SSZ-13.

It seems that $Pd^{2+}(CO)_2$ complex can be reduced to Pd(0) in a large extent shown by the large decreases in intensities of the doublet bands of this complex. This reduction leads to the appearance of the broad peak between 1800-2000 cm^{-1} that can be assigned to multi-bound CO on metallic Pd. The $Pd^{2+}(CO)_2$ complex is reformed with its entire initial IR intensity after re-oxidation, indicating that the Pd^{2+} ↔ Pd(0) cycle under dry condition is completely reversible. However, the $Pd^{2+}(OH)(CO)$ complex does not seem to reduce to Pd(0) under these conditions.

Since the earlier studies on Pd/zeolites have reported that dispersed Pd ions in zeolites are easily reduced and sintered into metallic Pd clusters by CO reduction,[46, 49] we tried to find the reason for non-reduced Pd ions in the above dry CO-TPR experiments. After saturating the oxidized (dehydrated) Pd/SSZ-13 with CO at 15°C, we followed the changes in the IR spectra as a function of time as water was injected onto the dehydrated zeolite sample (Figure S5). There is a sudden decrease in the intensities of IR bands representing $Pd^{2+}(CO)_2$ and $Pd^{2+}(OH)(CO)$, while a broad band of metallic Pd cluster-bound CO concomitantly appears at 1950 cm^{-1}. IR signals of gas phase CO_2 around 2350 cm^{-1} are also detected during the first few minutes. Such observations suggest that reduction of Pd ions can occur even at 15°C in the

presence of water. In the following wet CO-TPR (Figure 8), the amounts of CO consumed, and CO_2 formed largely increased. IR spectra also shows that both $Pd^{2+}(CO)_2$ and $Pd^{2+}(OH)(CO)$ can be fully reduced to metallic Pd(0) (Figure 8a). This means that the reduction of $Pd^{2+}(OH)(CO)$ complex requires the presence of H_2O. However, when this happens large Pd(0) "clusters" form as evidenced by the IR features at 1944 cm^{-1}, which is characteristic of CO bound to well defined metallic Pd particles in a bridged configuration. These clusters cannot be completely redispersed into cationic positions by the re-oxidation at 500°C as evidenced by the reduced intensities of the $Pd^{2+}(CO)_2$ complex in Figure 8. This process seems to yield larger PdO particles. Logically, Pd^{2+} ions bound to 2Al sites in zeolite framework cannot be reduced by CO. Only oxygen containing species like $Pd(OH)^+$ can be reduced to metallic Pd with the formation of CO_2 as described in previous studies.[17] If we assume that H_2O can hydrolyze Pd^{2+}/2Al sites into $Pd(OH)^+$/1Al and H^+/1Al sites, it is plausible to explain the results above: full reduction of Pd^{2+} can only occur for hydrated zeolite. However, further investigation will be needed to support this model. Note that fully reduced metallic Pd clusters can only partially recover to its initial state even after re-oxidation at 500°C (oxidation at even higher temperature may promote full dispersion of Pd^{2+} ions). In conclusion, the results presented in this part of the study clearly demonstrate that Pd^{2+} ions (present either as Pd^{2+} or $Pd(OH)^+$) in Pd/SSZ-13 PNA materials can be reduced to metallic Pd. Full reduction, however, requires the presence of H_2O and elevated samples temperatures.

3.5. Effects of H_2O on co-adsorption of CO and NO

The first step for activating hydrated Pd^{2+} ions is their coordination with CO ligands. To investigate this process CO adsorption was performed on hydrated Pd/SSZ-13 at 100°C (Figure S6). Note that Pd^{2+}-dicarbonyl cannot be observed at this high temperature due to its unstable nature as mentioned before. Main adsorption peaks under 150 ppm CO are found at 2134 and 2117 cm^{-1}, which can be assigned to Pd^{2+}-CO or $Pd^{2+}(OH)$-CO, respectively. The additional peaks at 2145 and 2161 cm^{-1} appear as the CO concentration increases to 2000 ppm. This indicates the formation of polycarbonyl Pd^{2+} species, analogous to the case of Pd/SSZ-39 that exhibited multiple peaks at 2163, 2153, and 2140 cm^{-1} under high CO pressure.[17] Based on these observations and the results discussed in the previous paragraphs, the role of $Pd^{2+}(NO)(CO)$ complex in passive NO storage is suggested in Figure 9. The adsorption of NO on hydrated Pd^{2+} ions is a slow process kinetically limiting the NO storage capacity in the presence of H_2O. In a CO+H_2O gas stream competition between CO and H_2O takes place resulting in the formation of a complex with mixed H_2O and CO ligands bound to the Pd^{2+} sites. However, once carbonyl Pd^{2+} species are formed they can be rapidly converted into $Pd^{2+}(NO)(CO)$ complex. The stability of the thus formed $Pd^{2+}(NO)(CO)$ complex depends on the adsorption conditions: it is stable in the presence of CO in the gas stream, or, in the absence of CO,

converts to $Pd^{2+}(NO)(H_2O)_x$. High temperature and low CO pressure can facilitate the desorption of CO. Thus, the critical role of CO is to provide an additional pathway for Pd^{2+}-NO formation with a lower energy barrier.

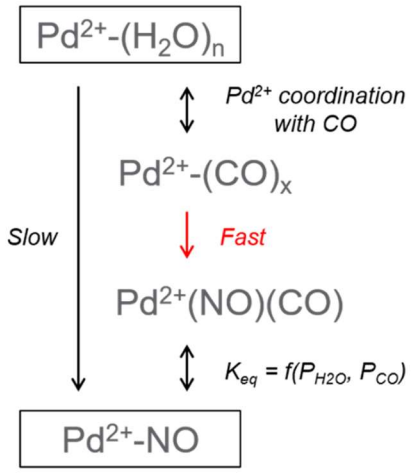

Figure 9. The suggested role of Pd^{2+}-CO-NO complex in activating hydrated Pd^{2+} ion into Pd^{2+}-NO.

Although the series of experiments discussed above can explain the role of CO in the promotion of NO uptake, one may consider another possibility, i.e., the role of a small amount of PdO clusters present in the 3 wt.% Pd/SSZ-13 sample and its effect on NO adsorption. To minimize the potential effect of the trace amount of PdO clusters, a 1 wt.% Pd/SSZ-13 sample was also tested under the same experimental conditions as the 3 wt.% one (Figures S7-S8). Like the high Pd loading sample, hydrated Pd^{2+} ions, which are ineffective for binding NO molecules, were activated by CO and form the same $Pd^{2+}(NO)(CO)$ complex observed in the high Pd loaded sample. Finally, we tested the promotional effect of CO on NO adsorption in a gas mixture containing NO, CO, and H_2O. After NO adsorption, the Pd/SSZ-13 was exposed to a gas stream containing 0.5% of H_2O (Figure 10a). The decrease in the intensity of the band at 1863 cm^{-1} coincided with a slight increase in the band at 1810 cm^{-1} after the initial 30s of H_2O exposure. This observation provides an evidence that the band centered at 1810 cm^{-1} assigned to Pd^{+}-NO has some additional components that can be promoted by water. One possibility is that part of this bands represents hydrated Pd^{2+}-NO species, which was observed in 1818 cm^{-1} in our studies at low (15°C) temperature. The other possibility is a $Pd^{2+}(OH)(NO)$ complex that can be formed by the hydrolysis of Pd^{2+}/2Al species. Our earlier calculation results suggested the 1804 cm^{-1} feature for Pd^{+}-NO, 1828 cm^{-1} for $Pd^{2+}(NO)(H_2O)$, and 1796 cm^{-1} for $Pd^{2+}(NO)(OH)$.[42] Due to their very similar peak positions, it is quite difficult to make exact

assignment for the nitrosyl band at 1810 cm^{-1} in this experiment. Regardless of their identity, the broad band at 1810 cm^{-1} lost some of its intensity upon exposure to H_2O due to formation of hydrated Pd^{2+} ions.

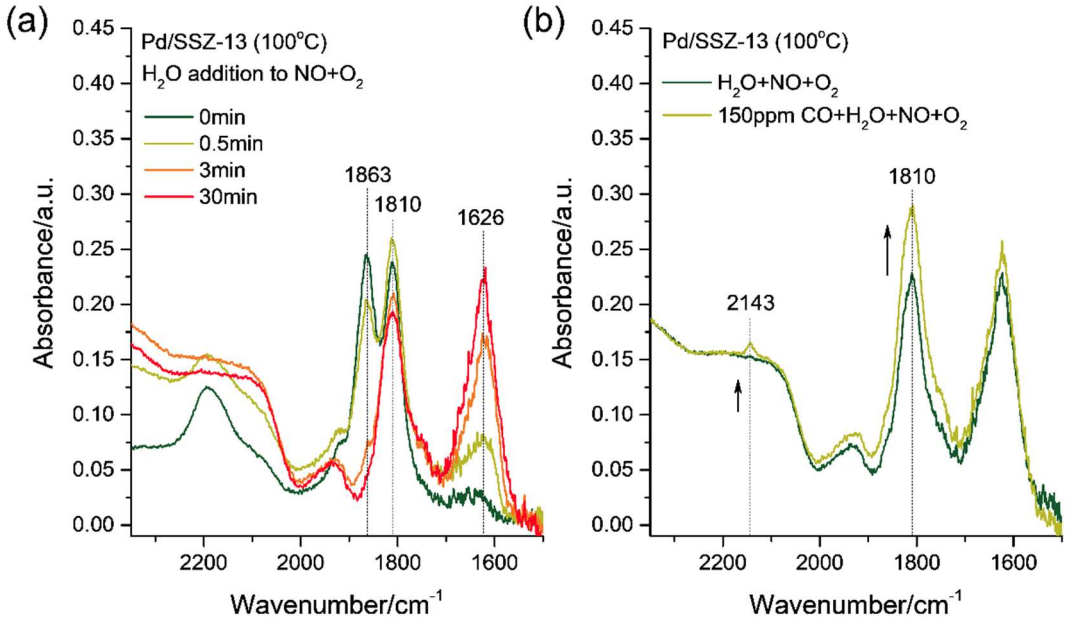

Figure 10. (a) Series of DRIFT spectra collected for Pd/SSZ-13 at 100°C after dehydration. 0.5% H_2O was added to $NO+O_2$ stream after NO adsorption under 200ppm NO + 1.5% O_2 at 100°C for 30min. Then, (b) 150ppm CO was added to $H_2O+NO+O_2$ feed.

Like the experiments under dry condition, the addition of 150 ppm CO abruptly increases the Pd^{2+}-NO bands centered at 1810 cm^{-1}, which is accompanied by the appearance of a small peak at 2143 cm^{-1} (Figure 10b). The peak at 2143 cm^{-1} is the clear evidence for the formation of $Pd^{2+}(NO)(CO)$ complex. In fact, several reports observed similar spectra in *in situ* IR experiments,[36-37] but the very small intensity of the 2143 cm^{-1} peak made it difficult to interpret. The small intensity of this band is simply due to the competitive coordination of H_2O and CO to Pd^{2+}-NO and the consequence that H_2O concentration is usually few percent while CO concentration is usually only few hundreds ppm. Although hydrated Pd^{2+} ions are activated via $Pd^{2+}(NO)(CO)$ complex, CO ligands can easily be displaced with H_2O. In fact, the IR features of $Pd^{2+}(NO)(CO)$ complex become much stronger by simply increasing the CO concentration (Figure S9). The removal of H_2O from the gas stream converts hydrated Pd^{2+}-NO to H_2O-free Pd^{2+}-NO species evidenced by the development of two peaks at 1863 and 1810 cm^{-1} (Figure S9). These peak positions are exactly the same as the ones we first observed in NO adsorption under dry condition in Figure 1. Thus, CO does not alter the chemical state of dispersed Pd^{2+} ions even in the presence of H_2O, if NO (and oxygen) is

present in the gas stream. However, water promotes the reduction of Pd^{2+} ions by CO even at the low temperature of 15°C (Figure 7-8). If Pd^{2+} ions are similarly reduced under PNA stream containing CO, NO, H_2O, and O_2, it is reasonable to think that NO adsorbed on metallic Pd should be dominantly observed. In this study, however, we always observe the peak of Pd^{2+}(NO) at 1863 cm^{-1} regardless of the presence or absence of CO. The simplest explanation is that NO or oxygen can prevent the reduction of Pd ions by CO. Further investigations would be needed to clarify this interesting phenomenon. Our work demonstrates that DRIFTS results are consistent with the IR results obtained in a static system by selecting proper experimental conditions. Also, clarification of the role of CO in NO storage will aid in the development of efficient PNA materials.

4. Conclusions

The promotion effect of CO on NO_x storage capacity of model Pd/SSZ-13 PNA materials was investigated with *in situ* DRIFTS. The formation of $Pd^{2+}(NO)(CO)$ complex was clearly observable at 100°C in dehydrated Pd/SSZ-13 and favored by increasing CO concentration in the PNA stream. However, the complex easily recovers to Pd^{2+}-NO in the absence of CO. For the hydrated Pd/SSZ-13 without pretreatment at high temperature, the addition of CO clearly increases the amount of stored NO mainly in the form of Pd^{2+}-NO, as well as small amounts of $Pd^{2+}(NO)(CO)$ complex. However, at low temperature where $Pd^{2+}(NO)(CO)$ complex is rather stable, the addition of CO distinctly increases the amount of NO storage only in the form of $Pd^{2+}(NO)(CO)$ complex. The conversion of Pd^{2+}-$(CO)_x$ to $Pd^{2+}(NO)(CO)$ is observed as a very fast process, and once formed the $Pd^{2+}(NO)(CO)$ complex can further decompose to Pd^{2+}-NO in the absence of CO. These observations can explain why $Pd^{2+}(NO)(CO)$ complex is important for activating hydrated Pd^{2+} ions into Pd^{2+}-NO species for NO storage in PNA. In addition, we found that the reduction of Pd^{2+} ions by CO is limited without water in the micropores of zeolite. The reduction of Pd^{2+} with CO is assisted by water and can occur even at the low temperature of 15°C. However, the Pd^{2+}-NO is always observed regardless of the presence or absence of CO, which led us to deduce that the reducing effect of CO would not satisfactorily explain the promoting role of CO in NO storage. Our findings are useful for understanding the facilitating role of CO on a wide range of other zeolite-based NO_x adsorption materials.

Acknowledgments

The authors gratefully acknowledge the US Department of Energy (DOE), Energy Efficiency and Renewable Energy, Vehicle Technologies Office for the support of this work. The research described in this paper was performed in the Environmental Molecular Sciences Laboratory (EMSL), a national scientific user facility sponsored by the DOE's Office of Biological and Environmental Research and located at Pacific Northwest National Laboratory (PNNL). PNNL is operated for the US DOE by Battelle.

References

1. Wang, A.; Olsson, L. The impact of automotive catalysis on the United Nations sustainable development goals. *Nat. Catal.* **2019,** 2 (7), 566-570.
2. Khivantsev, K.; Vargas, C. G.; Tian, J.; Kovarik, L.; Jaegers, N. R.; Szanyi, J.; Wang, Y. Economizing on Precious Metals in Three-Way Catalysts: Thermally Stable and Highly Active Single-Atom Rhodium on Ceria for NO Abatement under Dry and Industrially Relevant Conditions. *Angew. Chem.* **2021,** 133 (1), 395-402.
3. Kwak, J. H.; Tonkyn, R. G.; Kim, D. H.; Szanyi, J.; Peden, C. H. Excellent activity and selectivity of Cu-SSZ-13 in the selective catalytic reduction of NO_x with NH_3. *J. Catal.* **2010,** 275 (2), 187-190.
4. Kwak, J. H.; Kim, D. H.; Szailer, T.; Peden, C. H.; Szanyi, J. NO_x uptake mechanism on $Pt/BaO/Al_2O_3$ catalysts. *Catal. Lett.* **2006,** 111 (3), 119-126.
5. Lee, H.; Song, I.; Jeon, S. W.; Kim, D. H. Mobility of Cu Ions in Cu-SSZ-13 Determines the Reactivity of Selective Catalytic Reduction of NO_x with NH_3. *J. Phys. Chem. Lett.* **2021,** 12 (12), 3210-3216.
6. Gao, F.; Wang, Y.; Kollár, M.; Washton, N. M.; Szanyi, J.; Peden, C. H. A comparative kinetics study between Cu/SSZ-13 and Fe/SSZ-13 SCR catalysts. *Catal. Today* **2015,** 258, 347-358.
7. Gao, F.; Kwak, J. H.; Szanyi, J.; Peden, C. H. Current understanding of Cu-exchanged chabazite molecular sieves for use as commercial diesel engine $DeNO_x$ catalysts. *Top. Catal.* **2013,** 56 (15-17), 1441-1459.
8. Wang, A.; Chen, Y.; Walter, E. D.; Washton, N. M.; Mei, D.; Varga, T.; Wang, Y.; Szanyi, J.; Wang, Y.; Peden, C. H. Unraveling the mysterious failure of Cu/SAPO-34 selective catalytic reduction catalysts. *Nat. Commun.* **2019,** 10 (1), 1-10.
9. Song, I.; Lee, H.; Jeon, S. W.; Ibrahim, I. A.; Kim, J.; Byun, Y.; Koh, D. J.; Han, J. W.; Kim, D. H. Simple physical mixing of zeolite prevents sulfur deactivation of vanadia catalysts for NO_x removal. *Nat. Commun.* **2021,** 12 (1), 1-9.
10. Song, I.; Lee, H.; Jeon, S. W.; Kim, D. H. Controlling catalytic selectivity mediated by stabilization of reactive intermediates in small-pore environments: A study of Mn/TiO_2 in the NH_3-SCR reaction. *ACS Catal.* **2020,** 10 (20), 12017-12030.
11. Chen, H.-Y.; Collier, J. E.; Liu, D.; Mantarosie, L.; Durán-Martín, D.; Novák, V.; Rajaram, R. R.; Thompsett, D. Low temperature NO storage of zeolite supported Pd for low temperature diesel engine emission control. *Catal. Lett.* **2016,** 146 (9), 1706-1711.
12. Ryou, Y.; Lee, J.; Lee, H.; Kim, C. H.; Kim, D. H. Effect of sulfur aging and regeneration on low temperature NO adsorption over hydrothermally treated Pd/CeO_2 and $Pd/Ce_{0.58}Zr_{0.42}O_2$ catalysts. *Catal. Today* **2017,** 297, 53-59.
13. Khivantsev, K.; Jaegers, N. R.; Aleksandrov, H. A.; Song, I.; Hernandez, X. I. P.; Tian, J.; Kovarik, L.; Vayssilov, G. N.; Wang, Y.; Szanyi, J. Identification of single Ru(II) ions on ceria as a highly active catalyst for abatement of NOx pollutants. *Chemrxiv* **2021,** 10.33774/chemrxiv-2021-vr21g-v2.
14. Zheng, Y.; Kovarik, L.; Engelhard, M. H.; Wang, Y.; Wang, Y.; Gao, F.; Szanyi, J. n. Low-temperature Pd/zeolite passive NOx Adsorbers: structure, performance, and adsorption chemistry. *J. Phys. Chem. C* **2017,** 121 (29), 15793-15803.
15. Khivantsev, K.; Gao, F.; Kovarik, L.; Wang, Y.; Szanyi, J. n. Molecular Level Understanding of How Oxygen and Carbon Monoxide Improve NOx Storage in Palladium/SSZ-13 Passive NOx Adsorbers: The Role of NO^+ and Pd (II)(CO)(NO) Species. *J. Phys. Chem. C* **2018,** 122 (20), 10820-10827.
16. Lee, J.; Ryou, Y.; Cho, S. J.; Lee, H.; Kim, C. H.; Kim, D. H. Investigation of the active sites and optimum Pd/Al of Pd/ZSM–5 passive NO adsorbers for the cold-start application: evidence of isolated-Pd species obtained after a high-temperature thermal treatment. *Appl. Catal., B* **2018,** 226, 71-82.

17. Khivantsev, K.; Jaegers, N. R.; Kovarik, L.; Wang, M.; Hu, J. Z.; Wang, Y.; Derewinski, M. A.; Szanyi, J. The superior hydrothermal stability of Pd/SSZ-39 in low temperature passive NOx adsorption (PNA) and methane combustion. *Appl. Catal., B* **2021,** 280, 119449.
18. Khivantsev, K.; Wei, X.; Kovarik, L.; Jaegers, N. R.; Walter, E. D.; Tran, P.; Wang, Y.; Szanyi, J. Palladium/Ferrierite versus Palladium/SSZ-13 Passive NOx Adsorbers: Adsorbate-controlled Location of Atomically Dispersed Pd(II) in Ferrierite Determines High Activity and Stability. *Angew. Chem. Int. Ed.* **2021,** 10.1002/anie.202107554.
19. Cui, Y.; Zhu Chen, J.; Peng, B.; Kovarik, L.; Devaraj, A.; Li, Z.; Ma, T.; Wang, Y.; Szanyi, J.; Miller, J. T. Onset of High Methane Combustion Rates over Supported Palladium Catalysts: From Isolated Pd Cations to PdO Nanoparticles. *JACS Au* **2021,** 1 (4), 396-408.
20. Gao, F.; Szanyi, J. On the hydrothermal stability of Cu/SSZ-13 SCR catalysts. *Appl. Catal., A* **2018,** 560, 185-194.
21. Khivantsev, K.; Jaegers, N. R.; Kovarik, L.; Hanson, J. C.; Tao, F.; Tang, Y.; Zhang, X.; Koleva, I. Z.; Aleksandrov, H. A.; Vayssilov, G. N. Achieving Atomic Dispersion of Highly Loaded Transition Metals in Small-Pore Zeolite SSZ-13: High-Capacity and High-Efficiency Low-Temperature CO and Passive NOx Adsorbers. *Angew. Chem. Int. Ed.* **2018,** 57 (51), 16672-16677.
22. Jang, E. J.; Lee, J.; Oh, D. G.; Kwak, J. H. CH_4 Oxidation Activity in Pd and Pt–Pd Bimetallic Catalysts: Correlation with Surface PdO_x Quantified from the DRIFTS Study. *ACS Catal.* **2021,** 11 (10), 5894-5905.
23. Newton, M. A.; Belver-Coldeira, C.; Martínez-Arias, A.; Fernández-García, M. Dynamic in situ observation of rapid size and shape change of supported Pd nanoparticles during CO/NO cycling. *Nat. Mater.* **2007,** 6 (7), 528-532.
24. Okumura, K.; Kato, K.; Sanada, T.; Niwa, M. In-situ QXAFS studies on the dynamic coalescence and dispersion processes of Pd in the USY zeolite. *J. Phys. Chem. C* **2007,** 111 (39), 14426-14432.
25. Homeyer, S.; Sachtler, W. Oxidative redispersion of palladium and formation of PdO particles in NaY: An Application of High Precision TPR. *Appl. Catal.* **1989,** 54 (1), 189-202.
26. Pereira-Hernández, X. I.; DeLaRiva, A.; Muravev, V.; Kunwar, D.; Xiong, H.; Sudduth, B.; Engelhard, M.; Kovarik, L.; Hensen, E. J.; Wang, Y. Tuning Pt-CeO_2 interactions by high-temperature vapor-phase synthesis for improved reducibility of lattice oxygen. *Nat. Commun.* **2019,** 10 (1), 1-10.
27. Okumura, K.; Niwa, M. Regulation of the dispersion of PdO through the interaction with acid sites of zeolite studied by extended X-ray absorption fine structure. *J. Phys. Chem. B* **2000,** 104 (41), 9670-9675.
28. Ryou, Y.; Lee, J.; Cho, S. J.; Lee, H.; Kim, C. H.; Kim, D. H. Activation of Pd/SSZ-13 catalyst by hydrothermal aging treatment in passive NO adsorption performance at low temperature for cold start application. *Appl. Catal., B* **2017,** 212, 140-149.
29. Khivantsev, K.; Jaegers, N. R.; Kovarik, L.; Hu, J. Z.; Gao, F.; Wang, Y.; Szanyi, J. Palladium/zeolite low temperature passive NOx adsorbers (PNA): structure-adsorption property relationships for hydrothermally aged PNA materials. *Emission Contr. Sci. Technol.* **2020,** 6 (2), 126-138.
30. Lardinois, T. M.; Bates, J. S.; Lippie, H. H.; Russell, C. K.; Miller, J. T.; Meyer III, H. M.; Unocic, K. A.; Prikhodko, V.; Wei, X.; Lambert, C. K. Structural Interconversion between Agglomerated Palladium Domains and Mononuclear Pd (II) Cations in Chabazite Zeolites. *Chem. Mater.* **2021,** 33 (5), 1698-1713.
31. Khivantsev, K.; Jaegers, N. R.; Kovarik, L.; Prodinger, S.; Derewinski, M. A.; Wang, Y.; Gao, F.; Szanyi, J. Palladium/Beta zeolite passive NOx adsorbers (PNA): Clarification of PNA chemistry and the effects of CO and zeolite crystallite size on PNA performance. *Appl. Catal., A* **2019,** 569, 141-148.

32. Mei, D.; Gao, F.; Szanyi, J.; Wang, Y. Mechanistic insight into the passive NOx adsorption in the highly dispersed Pd/HBEA zeolite. *Appl. Catal., A* **2019,** 569, 181-189.
33. Gupta, A.; Kang, S. B.; Harold, M. P. NOx uptake and release on Pd/SSZ-13: Impact of Feed composition and temperature. *Catal. Today* **2021,** 360, 411-425.
34. Villamaina, R.; Iacobone, U.; Nova, I.; Tronconi, E.; Ruggeri, M. P.; Mantarosie, L.; Collier, J.; Thompsett, D. Mechanistic insight in NO trapping on Pd/Chabazite systems for the low-temperature NOx removal from Diesel exhausts. *Appl. Catal., B* **2021,** 284, 119724.
35. Mandal, K.; Gu, Y.; Westendorff, K. S.; Li, S.; Pihl, J. A.; Grabow, L. C.; Epling, W. S.; Paolucci, C. Condition-dependent Pd speciation and NO adsorption in Pd/zeolites. *ACS Catal.* **2020,** 10 (21), 12801-12818.
36. Lee, J.; Kim, J.; Kim, Y.; Hwang, S.; Lee, H.; Kim, C. H.; Kim, D. H. Improving NOx storage and CO oxidation abilities of Pd/SSZ-13 by increasing its hydrophobicity. *Appl. Catal., B* **2020,** 277, 119190.
37. Chen, Z.; Wang, M.; Wang, J.; Wang, C.; Wang, J.; Li, W.; Shen, M. Investigation of crystal size effect on the NOx storage performance of Pd/SSZ-13 passive NOx adsorbers. *Appl. Catal., B* **2021,** 291, 120026.
38. Kwak, J. H.; Varga, T.; Peden, C. H.; Gao, F.; Hanson, J. C.; Szanyi, J. Following the movement of Cu ions in a SSZ-13 zeolite during dehydration, reduction and adsorption: A combined in situ TP-XRD, XANES/DRIFTS study. *J. Catal.* **2014,** 314, 83-93.
39. Smith, L.; Cheetham, A.; Morris, R.; Marchese, L.; Thomas, J.; Wright, P.; Chen, J. On the nature of water bound to a solid acid catalyst. *Science* **1996,** 271 (5250), 799-802.
40. Jacobs, W.; Van Wolput, J.; Van Santen, R. An in situ Fourier transform infrared studyof zeolitic vibrations: Dehydration, deammoniation, and reammoniation of ion-exchanged Y zeolites. *Zeolites* **1993,** 13 (3), 170-182.
41. Sobalík, Z.; Dědeček, J.; Kaucký, D.; Wichterlová, B.; Drozdová, L.; Prins, R. Structure, Distribution, and Properties of Co Ions in Ferrierite Revealed by FTIR, UV–Vis, and EXAFS. *J. Catal.* **2000,** 194 (2), 330-342.
42. Khivantsev, K.; Jaegers, N. R.; Koleva, I. Z.; Aleksandrov, H. A.; Kovarik, L.; Engelhard, M.; Gao, F.; Wang, Y.; Vayssilov, G. N.; Szanyi, J. Stabilization of super electrophilic Pd^{+2} cations in small-pore SSZ-13 zeolite. *J. Phys. Chem. C* **2019,** 124 (1), 309-321.
43. Szanyi, J.; Kwak, J. H.; Zhu, H.; Peden, C. H. Characterization of Cu-SSZ-13 NH_3 SCR catalysts: an in situ FTIR study. *Phys. Chem. Chem. Phys.* **2013,** 15 (7), 2368-2380.
44. Khivantsev, K.; Kwak, J.-H.; Jaegers, N. R.; Derewinski, M. A.; Szanyi, J. Identification of the Mechanism of NO Reduction with Ammonia (SCR) on Zeolite Catalysts. *Chemrxiv* **2020,** 10.26434/chemrxiv.13134770.v1.
45. Khivantsev, K.; Vityuk, A.; Aleksandrov, H. A.; Vayssilov, G. N.; Blom, D.; Alexeev, O. S.; Amiridis, M. D. Synthesis, modeling, and catalytic properties of HY zeolite-supported rhodium dinitrosyl complexes. *ACS Catal.* **2017,** 7 (9), 5965-5982.
46. Aylor, A. W.; Lobree, L. J.; Reimer, J. A.; Bell, A. T. Investigations of the Dispersion of Pd in H-ZSM-5. *J. Catal.* **1997,** 172 (2), 453-462.
47. Kim, Y.; Hwang, S.; Lee, J.; Ryou, Y.; Lee, H.; Kim, C. H.; Kim, D. H. Comparison of NO_x Adsorption/Desorption Behaviors over Pd/CeO_2 and Pd/SSZ-13 as Passive NOx Adsorbers for Cold Start Application. *Emission Contr. Sci. Technol.* **2019,** 5 (2), 172-182.
48. Kim, Y.; Sung, J.; Kang, S.; Lee, J.; Kang, M.-H.; Hwang, S.; Park, H.; Kim, J.; Kim, Y.; Lee, E. Uniform synthesis of palladium species confined in a small-pore zeolite via full ion-exchange investigated by cryogenic electron microscopy. *J. Mater. Chem. A* **2021**.
49. Ryou, Y.; Lee, J.; Kim, Y.; Hwang, S.; Lee, H.; Kim, C. H.; Kim, D. H. Effect of reduction treatments (H_2 vs. CO) on the NO adsorption ability and the physicochemical properties of Pd/SSZ-13 passive NOx adsorber for cold start application. *Appl. Catal., A* **2019,** 569, 28-34.

Supplementary Information for

Elucidating the role of CO in NO storage mechanism on Pd/SSZ-13 with *in situ* DRIFTS

Inhak Song,[a] Konstantin Khivantsev,[a]* Yong Wang,[a,b] and János Szanyi[a]*

[a]Institute for Integrated Catalysis, Pacific Northwest National Laboratory, Richland, Washington 99352, United States

[b]Voiland School of Chemical Engineering and Bioengineering, Washington State University, Pullman, Washington 99164, United States

*Corresponding authors: konstantin.khivantsev@pnnl.gov and janos.szanyi@pnnl.gov

List of Supplementary Figures

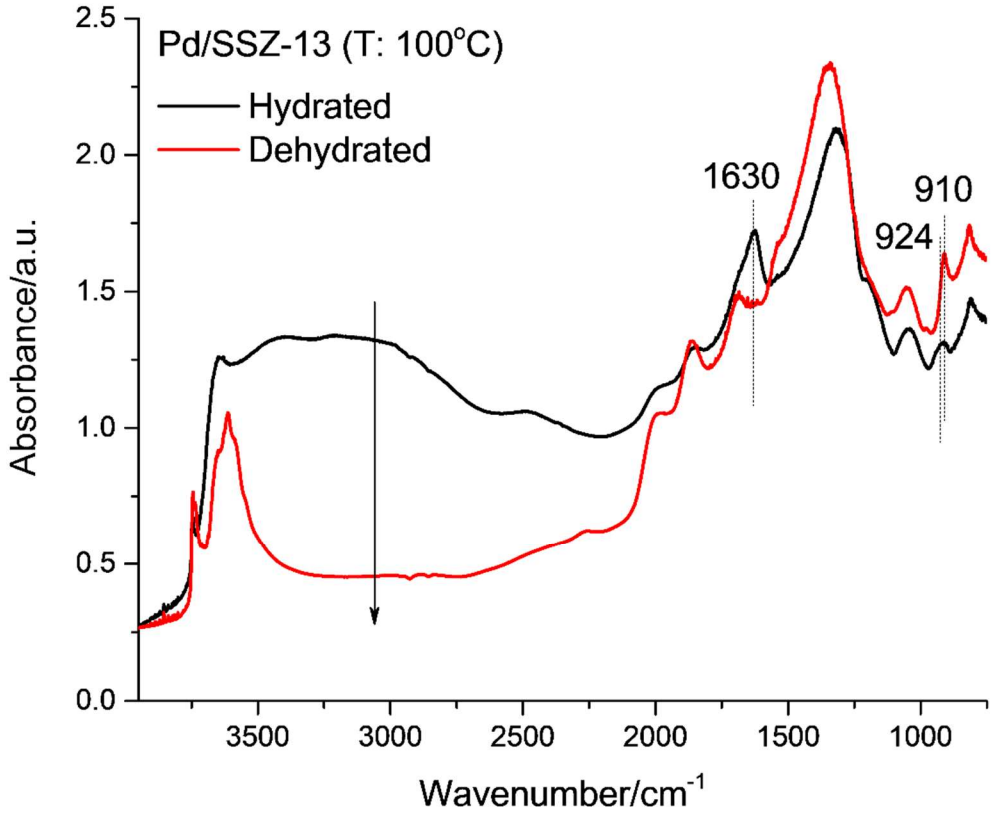

Figure S1. DRIFTS spectra of Pd/SSZ-13 collected at 100°C by using KBr background before and after dehydration (450°C under 1.5% O_2).

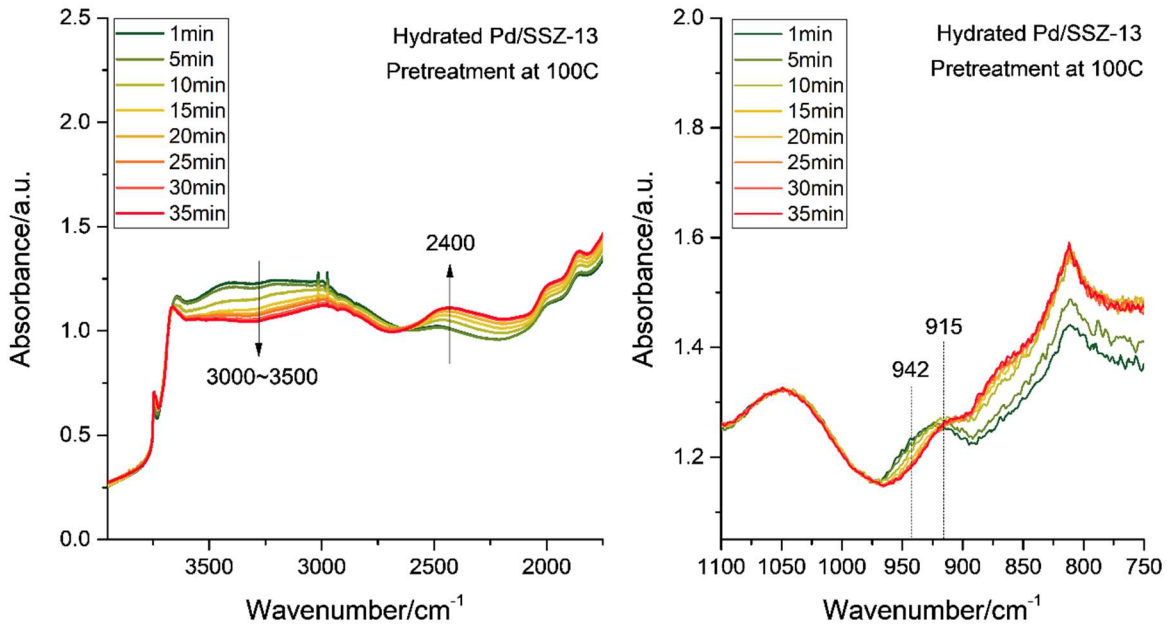

Figure S2. DRIFTS spectra of hydrated Pd/SSZ-13 during mild heat treatment at 100°C by using KBr background (under 1.5% O_2).

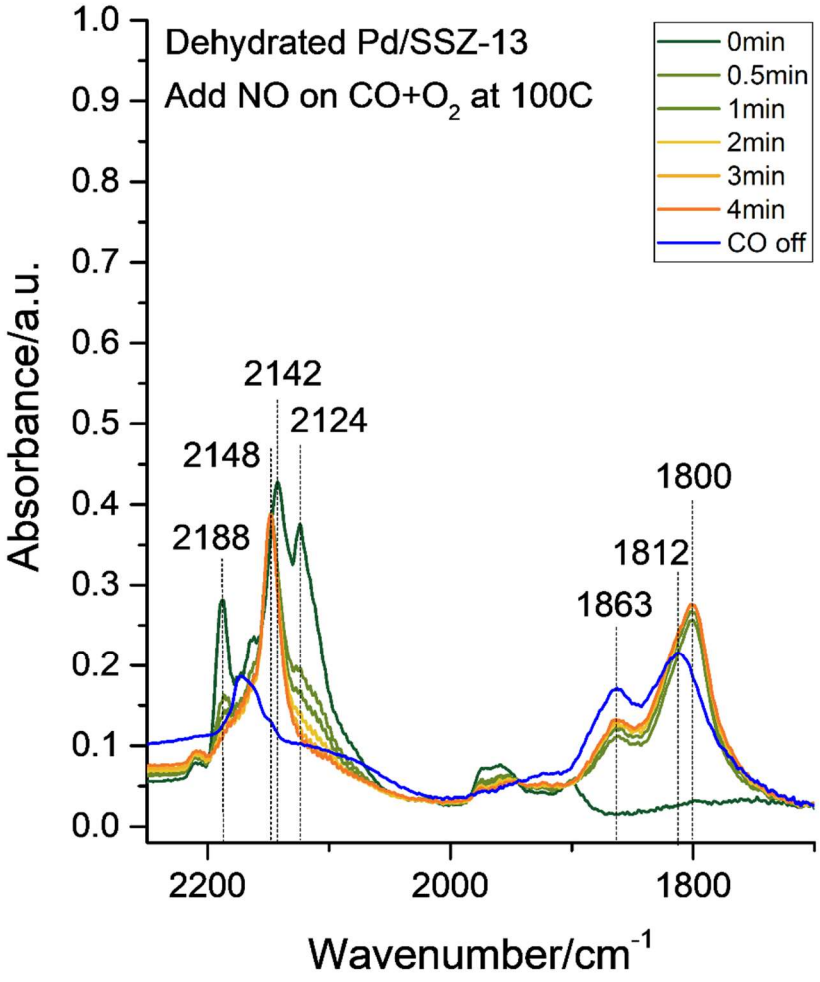

Figure S3. Series of DRIFTS spectra collected for Pd/SSZ-13 at 100°C after dehydration. 200ppm NO was added to the sample after CO adsorption under 2000ppm CO + 1.5% O_2 at 100°C.

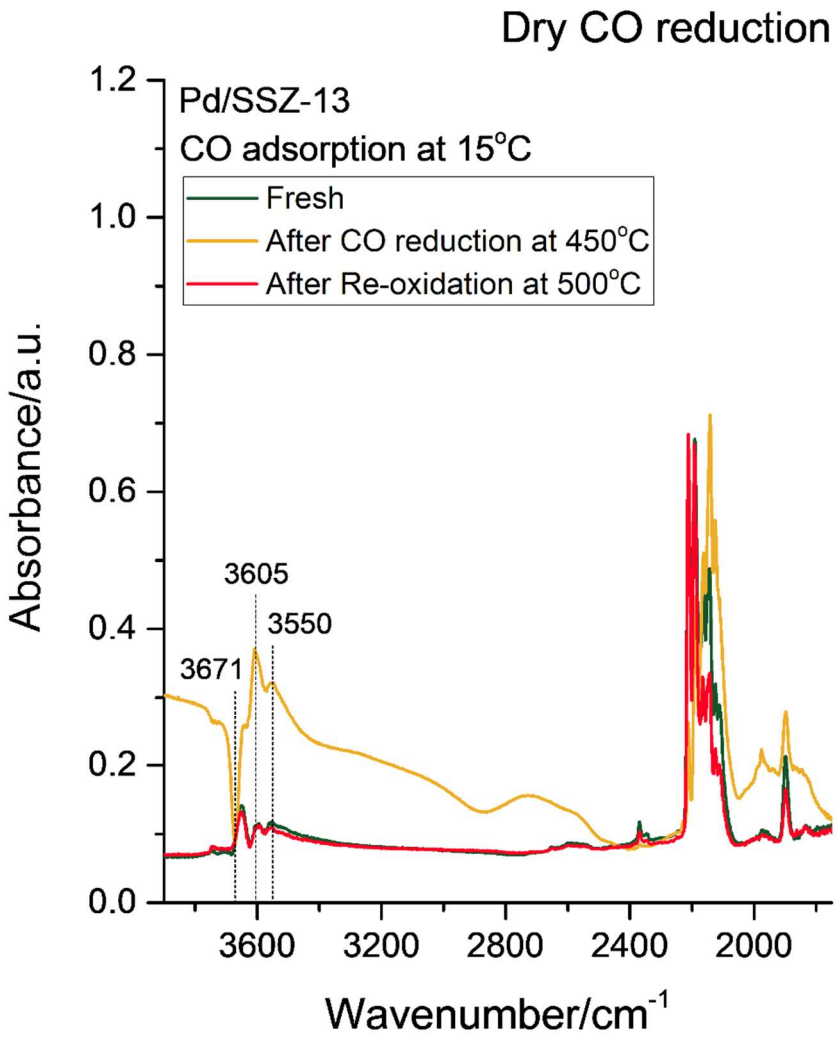

Figure S4. Effect of CO on dehydrated Pd/SSZ-13 was investigated by heating from 15 to 450°C under 2000ppm CO in DRIFTS-MS. The spectra were collected at 15°C after subsequent thermal treatments (2000ppm CO at 450°C, and 1.5% O_2 at 500°C).

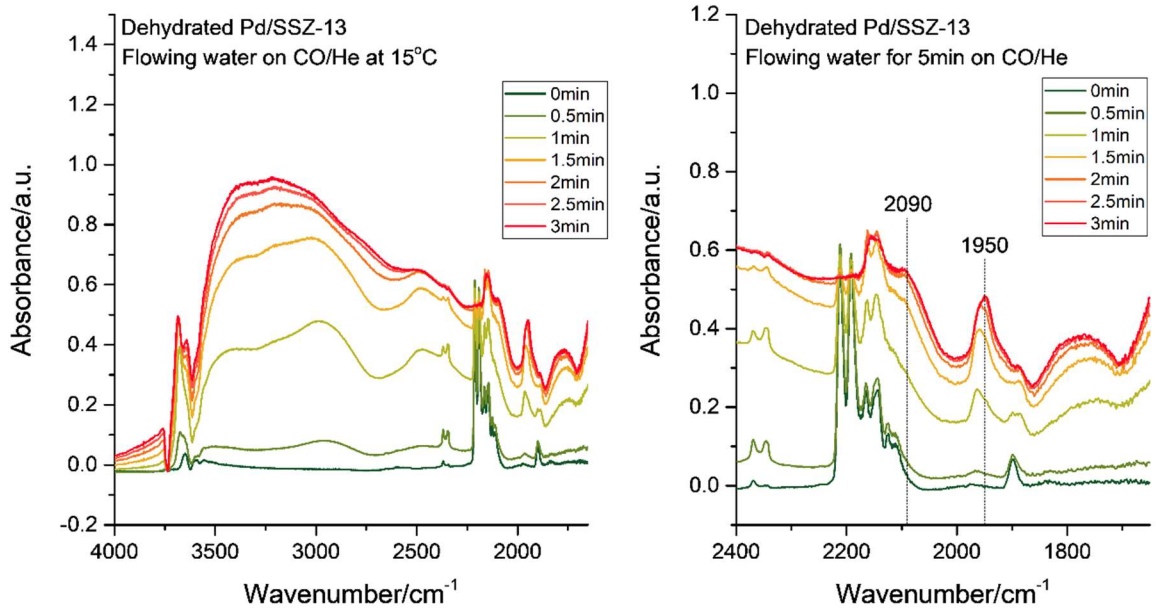

Figure S5. Series of DRIFTS spectra collected while saturating dehydrated Pd/SSZ-13 with H_2O at 15°C after pre-adsorption of CO. 0.5% H_2O was flowed for 5 min and then removed while continuously flowing 2000ppm CO/He to sample.

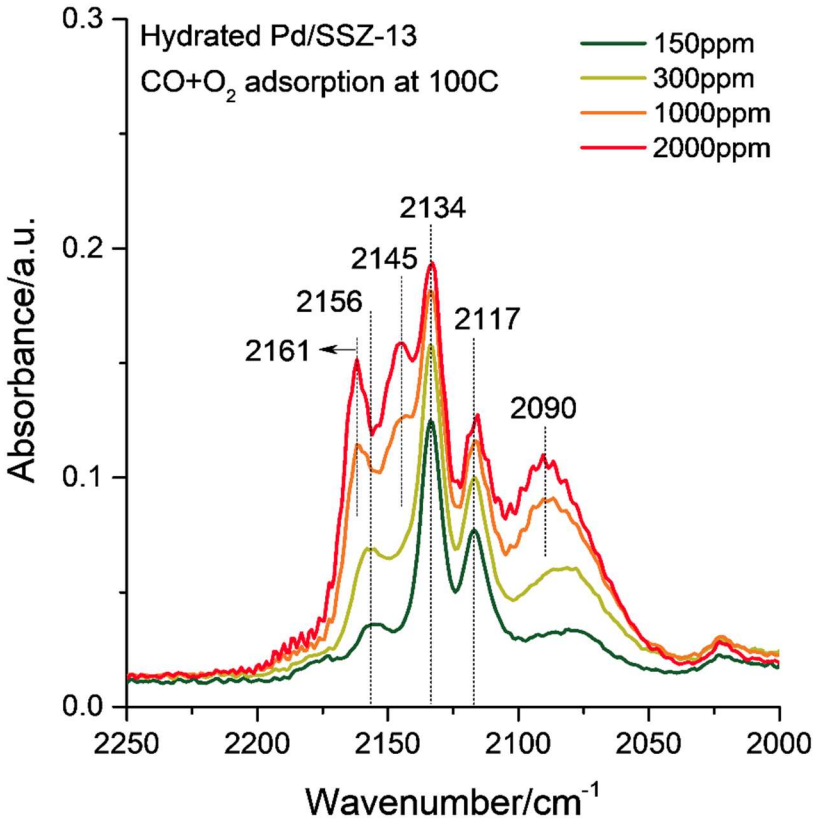

Figure S6. Series of DRIFTS spectra collected during $CO+O_2$ adsorption for hydrated Pd/SSZ-13 at 100°C.

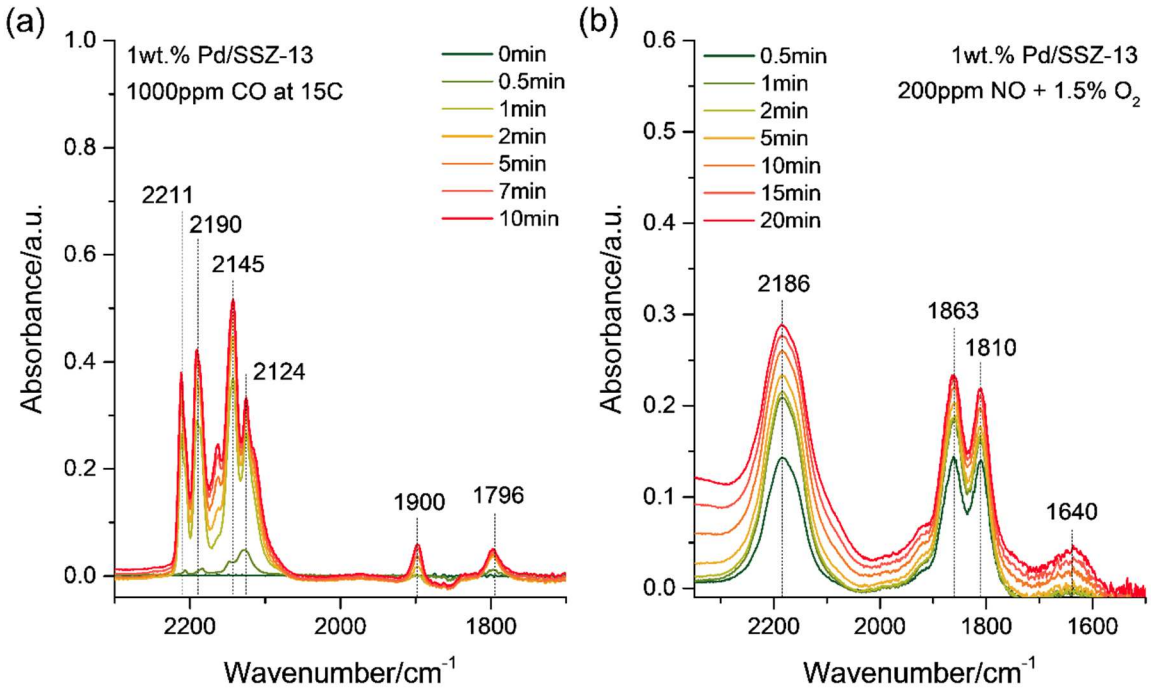

Figure S7. (a) Series of DRIFTS spectra collected at 15ºC during CO adsorption on dehydrated (500ºC, 1.5% O_2) 1 wt.% Pd/SSZ-13. (b) Spectra obtained during NO adsorption (200ppm NO, 1.5% O_2) at 100ºC on dehydrated 1 wt.% Pd/SSZ-13.

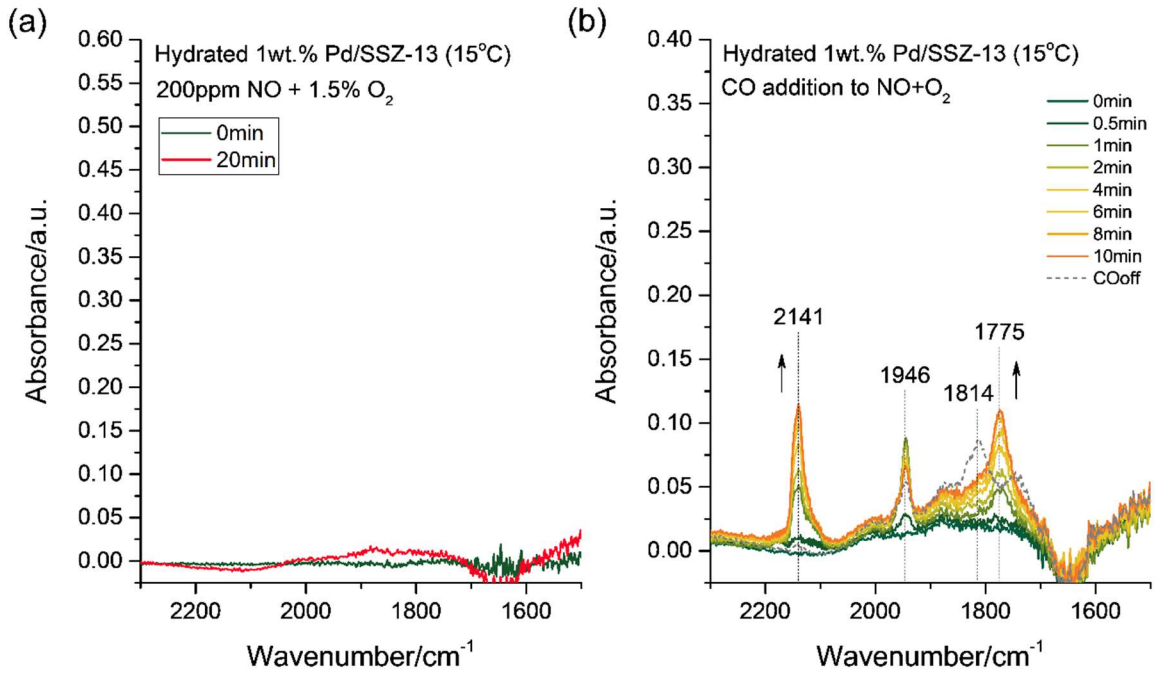

Figure S8. Series of DRIFTS spectra collected for hydrated 1 wt.% Pd/SSZ-13 at 15°C without dehydration. (a) Spectra obtained during adsorption of 200ppm NO + 1.5% O_2 at 15°C. Subsequently, (b) 1000ppm CO was added to NO+O_2 flow at same temperature.

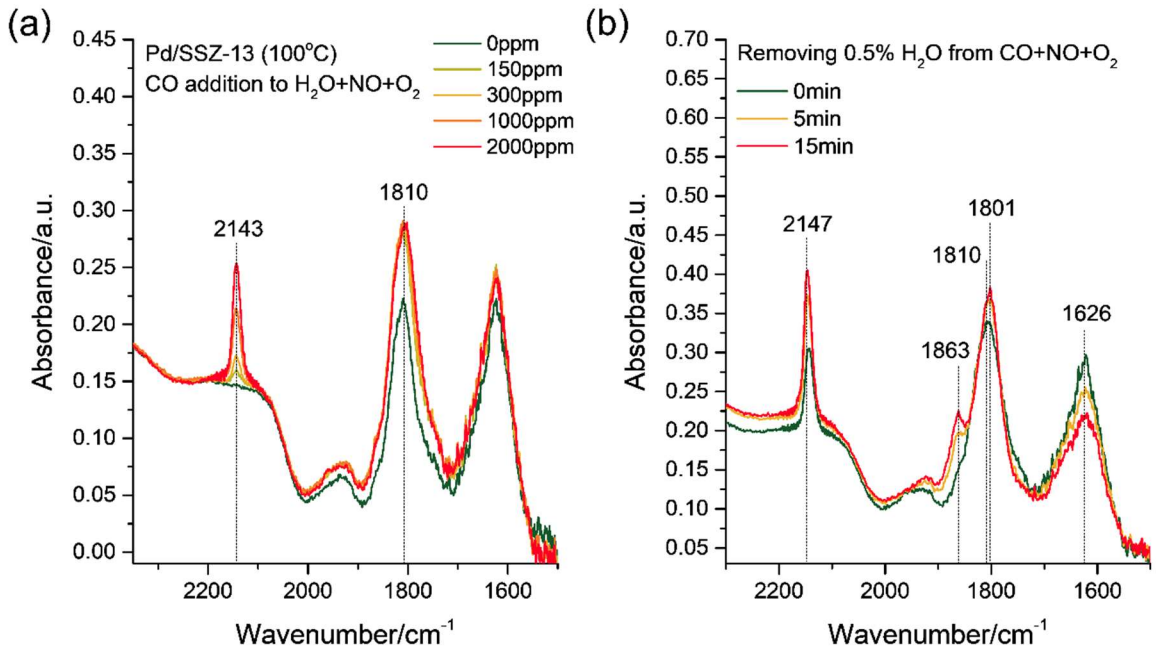

Figure S9. Series of DRIFTS spectra collected for Pd/SSZ-13 at 100°C. (a) After exposure to 0.5% H_2O, 200ppm NO, and 1.5% O_2, sample was exposed to CO with varying concentration from 150 to 2000 ppm. (b) Then, H_2O was removed from the gas feed.